# NSAUA 2024 Annual Meeting Abstracts – Basic Science

Cite as: *Can Urol Assoc J* 2024;18(9Suppl3):S174-8. http://dx.doi.org/10.5489/cuaj.8974

## Abstract 36

### Natriuretic peptide receptor 1 in the secretion of brain-derived neurotrophic factor by bladder smooth muscle cells

*Claudia Covarrubias[1], Philippe Cammisotto[1], Lysanne Campeau[1,2]*
[1]Lady Davis Institute for Medical Research, Montreal, QC; [2]McGill University, Montreal, QC

**Introduction:** Urine storage and voiding are controlled by the peripheral and central nervous systems. Neurotrophins are hormones essential for the maintenance and activity of nerves irrigating the bladder. A dysregulation in the ratio of brain-derived neurotrophic factor (BDNF) and its precursor (proBDNF) was observed in the urine of a female cohort with overactive bladder (OAB). Atrial natriuretic peptide (ANP) and nitric oxide (NO) levels in the same samples were found to be elevated. We herein examine the natriuretic peptide receptors (NPRs), NO, and cell pathways involved in the release of BDNF by bladder cells.

**Methods:** Primary cultures of rat bladder smooth muscle cells (SMCs) and urothelial cells (UROs) were incubated for 24 hours with natriuretic peptide A (ANP) (100 nM). ELISA kits were used to measure cyclic guanosine monophosphate (cGMP), cyclic adenosine monophosphate (cAMP), BDNF, and proBDNF. Matrix metalloproteinase-9 (MMP-9) activity was measured by enzymatic kinetics. NO was measured using the Griess method. Natriuretic receptor expression was measured by transcription polymerase chain reaction (RTqPCR) after Clustered Regularly Interspaced Short Palindromic Repeats (CRISPR)-Cas9 genomic edition.

**Results:** SMCs are a major source of BDNF and proBDNF while urothelial cells (UROs) secrete most of the MMP-9, the enzyme converting proBDNF into mature BDNF, as confirmed by deletion of MMP-9 using CRISPR-Cas9. Incubation of SMCs with ANP (100 nM) for 24 hours decreased secretion of proBDNF and increased that of BDNF. ANP only increased the secretion of MMP-9 in UROs. Knockdown of the natriuretic peptide receptor 1 (NPR-1) gene by CRISPR-Cas9 plasmid completely abolished the increase in BDNF secretion elicited by ANP. On the other hand, an increase in cGMP was triggered by ANP and followed by an increase in cAMP levels. Dibutyryl cAMP (500 µM) by itself mimicked the effect of ANP by increasing BDNF secretion and MMP-9 proteolytic activity. In parallel, ANP incubation led to a decrease in NO content, and L-NAME, a nitric oxide synthase (NOS) enzyme inhibitor, increased BDNF secretion but decreased MMP-9.

**Conclusions:** These data suggest that in SMCs, ANP controls the secretion of BNDF and its precursor by binding NPR-1 involving at least two different pathways; one requiring an increase in cGMP, and the other a decrease in NO synthesis. ANP also increases the secretion of MMP-9 from UROs, enhancing the conversion of proBDNF to mature BDNF.

**Funding:** Canadian Urological Association

## Abstract 37

### CRISPR-Cas9 deletion of matrix metalloproteinase-9 improved bladder contraction in an animal model of diabetic voiding dysfunction

*Philippe Cammisotto, Lysanne Campeau*
Lady Davis Institute for Medical Research, Montreal, QC

**Introduction:** Peripheral and central nervous systems control relaxation and contraction of the bladder wall. Neurotrophins are essential in the maintenance and activity of nerves irrigating the bladder. Among them, nerve growth factor (NGF) promotes neuroregeneration by binding receptor TrkA, while its precursor, proNGF, triggers inflammation and apoptosis through receptor p75NTR. Rodent models of diabetes (types 1 and 2) characterized by voiding dysfunction and treated with THX-B, a p75NTR antagonist, display improved bladder parameters through reduction of matrix metalloproteinase-9 (MMP-9), the major protease involved in NGF proteolysis. In the present study, we used a Clustered Regularly Interspaced Short Palindromic Repeats (CRISPR)-Cas9 plasmid *in vivo* to target MMP-9 gene specifically in the urothelium.

**Methods:** Bladders of female Tally Ho mice (aged five months) in prediabetic state (glycemia between 7 and 14 mM) were transfected with CRISPR-Cas9 plasmid targeting MMP-9 gene. Voiding spot assays were performed weekly to measure urine volume, spot number, and volume/spot. Bladders were taken for analysis of NGF and proNGF by ELISA; and MMP-9 and markers of nerve endings, Vacht, and pgp9.5 by semi-quantitative immunoblotting. Bladder strip contraction was measured in organ baths. Histology was carried out to observe bladder wall morphology. T-test and ANOVA were used for statistics.

**Results:** Two weeks after transfection: glycemia, body weight, and ratio bladder mass/body weight were similar between the groups. Urine volume increased in the sham group by 195% while it decreased by 39% with MMP-9 knockdown ($P<0.01$). Number of spots were increased in the sham group (+27%) and decreased in the CRISPR group (-21%, $P<0.05$). Volume/spot were not statistically different. Immunoblotting showed that MMP-9 urothelial content was decreased by 63% ($P<0.001$) after transfection, which led to an increase in NGF (+192%, $P<0.01$). ProNGF was unchanged, and the ratio of NGF/proNGF increased by 250% ($P<0.01$). Vacht expression decreased by 55% while pgp9.5 was unaffected. Contractions of bladder strips elicited by KCl (120 mM), EFS (1–32 Hz), and carbachol (3 nM–100 microM) decreased by 41%, 69%, and 39% respectively. Finally, histologic examination of tissues did not reveal signs of inflammation or changes in bladder wall structure and thickness.

**Conclusions:** MMP-9 appears to be central in the control of bladder contraction through increases in the ratio of NGF/proNGF. MMP-9 inhibition might constitute an interesting avenue for correcting bladder dysfunction.

**Funding:** Quebec Network for Research on Aging

## Abstract 39

### Impact of TRAP1 on complex II assembly in cells with pathogenic familial pheochromocytoma-associated mutations

*Nathan Nahhas, Ariba Khan, Julia K. Burckacki, Gianna L. Mochi, Mark R. Woodford*
SUNY Upstate Medical University, Department of Urology, Syracuse, NY

**Introduction:** The succinate dehydrogenase enzyme (SDH) is integral to the oxidative phosphorylation pathway and has been found to play a role in tumor oncogenesis and metabolism. SDH loss of function mutations are associated with pheochromocytomas and paragangliomas. Germline mutations have also been associated with familial tumor syndromes. No targeted pharmaceutical therapies are available for these tumors. The mitochondrial chaperone TNF-receptor associated protein 1 (TRAP1) and SDH assembly factor 2 (SDHAF2) have been shown to participate in SDH complex assembly, but their functional pathways are not fully elucidated. TRAP1 expression is upregulated in multiple cancer models, and previous work has shown that inhibition of TRAP1 induces apoptosis in tumor cells. The objective of our work was to determine the mechanism of uncharacterized pathogenic SDH and SDHAF2 mutations, and the role of TRAP1 in this process.

**Methods:** DNA plasmid transfection of mutants clinically associated with pheochromocytoma in 293 wild type and succinate dehydrogenase B (SDBH) subunit knockout cells was used to modulate levels of SDHB and SDHAF2 proteins. Immunoblotting and immunoprecipitation were used with submitochondrial fractionation to evaluate protein expression and interaction in the setting of TRAP1 drug inhibition. *In vitro* enzymatic assays and real-time respiratory assays were used to evaluate SDH activity.

**Results:** SDHB mutation resulted in impaired binding to the SDHA subunit and failed to rescue respiratory function compared to wild type. The pathogenic SDHAF2-G78R mutant also exhibited reduced binding to SDHA and decreased SDH activity *in vitro*. Interestingly, we were not able to observe interaction between

TRAP1 and SDHAF2. Further, TRAP1 knockout compromised binding between SDHAF2 and SDHA. This indicated that TRAP1 is unable to incorporate pathogenic mutant proteins into functional SDH complexes.
**Conclusions:** TRAP1 has a regulatory role in assembly of functional SDH complexes, and TRAP1 binding has been shown to inhibit the function of SDH. However, TRAP1 fails to bind with pathogenic mutations of SDHB, leading to a lack of respiratory function. In both TRAP1 knockout and pathogenic SDHAF2 mutations, SDH complexes fail to assemble, suggesting that TRAP1 and SDHAF2 are both required for SDH complex function. Our data suggests TRAP1 and SDHAF2 act in a mutually exclusive manner for SDH complex assembly. As TRAP1 regulates respiratory function, TRAP1 modification therapy could be explored for patients with familial pheochromocytoma syndrome or tumors with metabolic SDH dysregulation.
**Funding:** N/A

## Abstract 40

### Histological patterns and recurrence of Hunner lesions in interstitial cystitis/bladder pain syndrome and effectiveness of triamcinolone injection

*Hend Alshamsi[1], Claudia Covarrubias[2], Philippe Cammisotto[2], Lysanne Campeau[1]*
[1]Urology Department, McGill University, Montreal, QC; [2]Lady Davis Institute for Medical Research, McGill University, Montreal, QC

**Introduction:** Interstitial cystitis/bladder pain syndrome (IC/BPS) is a chronic, debilitating condition affecting the bladder and surrounding tissues. It is believed to involve abnormalities in the bladder lining as well as the immune and nervous systems. It can present with Hunner lesions (HL) which feature areas of inflammation and ulceration, causing severe pain and bleeding. Treatment of HL includes fulguration and/or injection of triamcinolone. This study aims to examine the histopathology and immunostaining of HL and investigate its impact on the severity, progression, recurrence rate, and response to triamcinolone in those who received it.
**Methods:** A retrospective chart review was conducted of 14 patient demographics (median age of 65.66±16.15 years), clinical characteristics, and treatment outcomes for patients with HL, non-Hunner lesions (NHL), and unaffected controls (UC) who were treated from January 2013 to November 2023. Bladder biopsies were stained with hematoxylin and eosin (H&E) and with antibodies (p75NTR, TNF-alpha, CD68, and E-Cadherin). Data was statistically analyzed using GraphPad Prism 9 software.
**Results:** This study comprised a total of 14 participants who were monitored for an average duration of six years (one–16.9 years). Bladder biopsies were obtained from 13 out of the 14 individuals (12 females, one male) with HL IC/BPS (n=6), NHL IC/BPS (n=3), and UC (n=4). The number and location of HL varied among patients, ranging from one to six lesions, predominantly located at the dome, posterior, and posterolateral walls. All patients with HL underwent various therapies, including medical oral therapy (4/5 patients) and fulguration (4/5 patients). Among the patients with HL, five out of seven (71.4%) received intravesical injection of triamcinolone at the lesion sites, with three patients requiring multiple re-treatments (up to 3–6 times) due to symptom recurrence. One out of the seven patients underwent simple cystectomy without a triamcinolone injection trial. Histopathological analysis revealed acute and chronic inflammatory changes along with extensive denudation in the HL group, exhibiting more mast cells and fibrosis in the subgroup that received multiple triamcinolone injections. Preliminary results of immunostaining indicated cells positive for TNF-alpha, CD 68, and receptor p75NTR in the lamina propria HL samples as compared to those with NHL and UC.
**Conclusions:** Individuals diagnosed with IC/BPS with HL who undergo treatment with triamcinolone have higher recurrence rates and display more pronounced clinical manifestations, pathological features, and positive immunostaining for TNF-alpha, CD68, and p75NTR when compared to patients with NHL and UC. Further investigations with a larger patient cohort are imperative to validate these observed results.
**Funding:** N/A

## Abstract 41

### YAP/TAZ expression correlates with degree of tumor fibrosis in clear cell renal cell carcinoma

*Asef Aziz[1], Nusret Subasi[2], Shreya Patel[2], Andrea Lightle[2], Rauf Shahbazov[3], Mahmut Akgul[2], Rohan Samarakoon[4], Barry Kogan[1]*
[1]Albany Medical Center, Department of Urology, Albany, NY; [2]Albany Medical Center, Department of Pathology, Albany, NY; [3]Albany Medical Center, Department of Surgery, Albany, NY; [4]Albany Medical Center, Department of Regenerative Cancer Cell Biology, Albany, NY

**Introduction:** The Hippo pathway, consisting of the nuclear tranducers Yes-associated protein (YAP) and transcriptional coactivator with PDZ-binding motif (TAZ), controls organ size by regulating cell proliferation, differentiation, and apoptosis. Hyperactivation of the pathway in the tumor microenvironment contributes to the progression of various solid tumors including clear cell renal cell carcinoma (ccRCC). Recent studies have suggested that intra- and peri-tumoral fibrosis contribute to disease progression in ccRCC. As interstitial YAP and TAZ overexpression has been shown to contribute to the development of fibrosis in benign kidney, we hypothesized that YAP/TAZ expression would increase with levels of intra- and peri-tumoral fibrosis in ccRCC.
**Methods:** Tissue microarrays (TMAs) were constructed from 60 tissue samples of patients who underwent radical or partial nephrectomy for ccRCC. Demographic data and medical history were collected retrospectively. Degree of fibrosis in the peri-and intra-tumor tissue was graded and classified as none (0–5%), mild (5–25%), moderate (26–50%), or severe (>50%). TMAs were evaluated for expression of YAP and TAZ by immunohistochemical (IHC) staining. Extent (0–100%) of YAP/TAZ staining in the intra-tumor fibrotic region and peri-tumor tissue was blindly scored. YAP/TAZ expression relative to fibrosis in the various tissue regions was compared.
**Results:** The population had a median age of 65 years and mostly identified as Caucasian (94%) males (65%). Tumor characteristics were similar in compared cohorts. In both the peri-tumor [none (n=19, 0±0); mild (n=10, 11±12.0); moderate (n=11, 15±14.7); and severe (n=15, 45±25); p<0.0001] and intra-tumor fibrotic regions [none (n=20, 0±0); mild (n=22, 8.6±13.0); moderate (n=15, 14±18.3); and severe (n=3, 23.3±20.8); p<0.01] extent of YAP/TAZ staining was significantly increased with increased degree of fibrosis.
**Conclusions:** YAP/TAZ expression appears to corelate with degree of tumoral fibrosis in ccRCC. Our findings suggest that these Hippo transducers contribute to development or progression of intra-tumoral and peri-tumoral fibrosis.
**Funding:** N/A

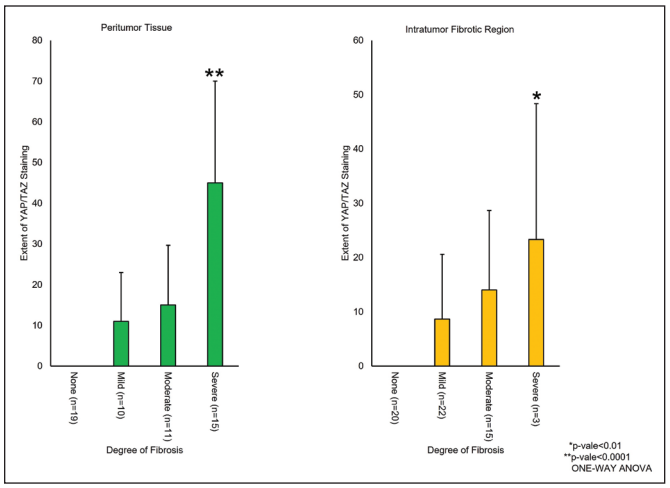


**Abstract 41. Figure 1.** Extent of YAP/TAZ staining in peritumor tissue and intra-tumoral fibrotic region correlates with degree of fibrosis in the region.

## Abstract 42

### Regulation of CDK4/6 axis signaling by PP5 and its role in bladder cancer

*Rebecca A Sager, Sarah J Backe, Michael Basin, Joseph Jacob, Mark R Woodford, Gennady Bratslavsky, Mehdi Mollapour*

Department of Urology, Upstate Medical University, Syracuse, NY

**Introduction:** Bladder cancer (BCa) has the highest recurrence rate of any solid cancer with limited therapeutic options and few targeted therapies for advanced disease. Loss of cell cycle control is a hallmark of cancer, and alterations in the regulatory cyclin dependent kinase 4/6 (CDK4/6)-retinoblastoma (Rb) axis are frequent in BCa. CDK4 and CDK6 regulate cell cycle progression through phosphorylation of the tumor suppressor Rb. The tumor suppressor p16 provides inhibitory control of CDK4/6 activity and is frequently lost in BCa. Specific inhibitors of CDK4/6 (CDK4/6i) are approved in breast cancer and have been investigated in BCa. CDK4/6i monotherapy had limited efficacy in platinum-refractory disease. Many studies highlight the need for better patient selection and rational combinations. Protein phosphatase 5 (PP5) is best known for its role in the chaperoning of kinases, including CDK4. PP5 is upregulated in BCa and is associated with poor survival. PP5 knockdown (KD) led to G0/G1 arrest in BCa cells, suggesting impairment of progression to S-phase, the key step controlled by CDK4/6. We sought to determine the role of PP5 in regulation of CDK4/6 signaling and the effect on sensitivity to CDK4/6i in BCa.

**Methods:** We utilized data in cBioPortal to examine alteration type and frequency in PPP5C as well as CDK4/6 axis members. The effect of PP5 activity on CDK4/6 axis signaling was examined using Western blot, immunoprecipitation, and mRNA expression assays in normal and BCa cell lines. The effects of PP5 KD and CDK4/6i treatment on BCa cells were assessed by cell viability and colony formation assays as well as cell cycle analysis by flow cytometry.

**Results:** We identified PP5 mRNA upregulation in 17% of muscle-invasive BCa specimens, and PP5 alteration was associated with worse overall survival. We further found that PP5 exists in complex with both CDK4 and the tumor suppressor p16. Overexpression or KD of PP5 leads to significant changes in CDK4/6 axis signaling. Additionally, PP5 KD decreased the growth of BCa cells and enhanced the effect of the CDK4/6i palbociclib on growth inhibition and cell cycle arrest.

**Conclusions:** PP5 is frequently upregulated in BCa, and KD leads to decrease in BCa cell viability and to cell cycle arrest. PP5 controls the cell cycle through interactions with CDK4 and p16 and affects downstream signaling of this key pathway. PP5 KD enhances the effect of treatment with CDK4/6i in BCa cells. Combination therapy of PP5 inhibition and CDK4/6i in BCa should be examined further.

**Funding:** This work was supported in part by the 2022 Urology Care Foundation Residency Research Award Program (RAS) and the Kahlert Foundation.

## Abstract 43

### Polymyxin B irrigation fluid vs. uropathogenic *E. coli* in a benchtop ureteroscopy model

*Stephen Hassig[1], Yixi Hu[1], Shu-Yuan Yeh[1], Scott Quarrier[1], Dirk Lange[2], Brian Eisner[3,4], Rajat Jain[1]*

[1]University of Rochester Medical Center, Rochester, NY; [2]Vancouver Coastal Health Research Institute, Vancouver, BC; [3]Massachusetts General Hospital, Boston, MA; [4]Harvard Medical School, Boston, MA

**Introduction:** Serious infections after ureteroscopy are increasing with significant morbidity, mortality, and financial costs. Aside from preoperative antibiotics and intrarenal pressure reduction, little is done to address stone-associated pathogen burden within the kidney, with current standard of care utilizing saline irrigation. Polymyxin B (PMB) is a gram-negative bactericidal peptide that, uniquely, neutralizes sepsis-inducing lipopolysaccharide (LPS). Though dose-limited via IV due to toxicities, PMB has never been used in ureteroscopic irrigation fluid. We hypothesize that PMB will reduce viable bacteria in a bench renal irrigation model at doses below typical IV doses.

**Methods:** ATCC CFT073 uropathogenic *E. coli* were incubated to 0.35 OD600, or about 2.4 x 108 cells per mL. Two mL were added to a stoppered 5 mL test tube. The stopper was penetrated with a 16 g needle for inflow of irrigation (approximating the 3.6 fr irrigation channel in many ureteroscopes) and a 14 g angiocath for outflow of the closed system (approximating the area available for outflow between a 9.5 fr scope and an 11/13 fr ureteral sheath). Bags of 250 cc 0.9% saline containing 0 units (control), 5000 units, 10 000 units, and 20 000 units of PMB were irrigated through the tube over 15 minutes (rate: 1 L/hour). Fifteen microliter effluent samples were obtained and plated at time 0, 30 seconds, 1 minute, 3 minutes, 7 minutes, 10 minutes, and 15 minutes. At completion, test tubes were emptied, 1 mL of broth was added, and tubes were incubated for one hour and then plated.

**Results:** Numerous colonies grew throughout all time points for the saline control. The 5000 unit trial had lawn growth at time 0, 88 colonies at 30 seconds, 25 colonies at one minute, 15 colonies at 3 minutes, and then no growth for the remainder. The 10 000 unit trial had lawn growth at time 0 followed by no growth throughout. Lastly, the 20 000 unit trial had one colony at time 0 followed by no growth throughout. For tube culturing, the saline control tube demonstrated lawn growth followed by 71 colonies from the 5000 unit tube, and no colonies from the 10 000 and 20 000 unit tubes. Irrigation fluid was visually clear across all doses.

**Conclusions:** PMB irrigation clears significant *E. coli* burden at doses far below the IV dose (15 000–25 000 units/kg/day) in a benchtop renal irrigation model. Next steps include assessing LPS reduction in this model and ultimately tolerability and efficacy in an animal model.

**Funding:** N/A

## Abstract 44

### Durably infected kidney stone model with viable internal and external *E. coli*

*Stephen Hassig[1], Yixi Hu[1], Shu-Yuan Yeh[1], Scott Quarrier[1], Dirk Lange[2], Brian Eisner[3,4], Rajat Jain[1]*

[1]University of Rochester Medical Center, Rochester, NY; [2]Vancouver Coastal Health Research Institute, Vancouver, BC; [3]Massachusetts General Hospital, Boston, MA; [4]Harvard Medical School, Boston, MA

**Introduction:** Infectious complications following ureteroscopy are common and can lead to significant morbidity and death. Clinical research is ongoing, but bench research is stifled by the lack of a robust bench top model for infected kidney stones. We present a straightforward method for reproducible production of an *in vitro* kidney stone phantom inoculated with uropathogenic *E. coli.*

**Methods:** ATCC CFT073 uropathogenic *E. coli* were incubated to an optical density of 0.35 (OD600) or about 2.4 x 108 cells/mL, and 10 mL were centrifuged at 1500 RCF for 10 minutes. The pellet was resuspended in 0.9% saline or sterile water. This was then added to varying amounts of BegoStone Plus and powdered egg albumin. The slurry was poured into cylindrical molds to set. At 24 hours, intact and crushed cylinders were added to 1 mL of Luria Broth (LB), while a subset were immersed in 70% ethanol for 5, 10, 15, and 20 minutes followed by LB rinse. This was repeated at 48 hours with dry storage in the mold at room temperature. Separately, previously made phantoms were inoculated with 1 mL of *E. coli* for one hour. Stones were then rinsed with LB to remove any residual bacteria-laden media and subjected to 15 minutes of ethanol, 20 minutes under UV light (agitated every 5 minutes), or steam autoclave. Each was then incubated for 1 hour in LB and plated.

**Results:** Growth was demonstrated on plates from intact and crushed BegoStone-albumin-*E. coli* stones at 24 and 48 hours. Growth was reduced from intact stones that were immersed in ethanol for five minutes, with cultures from stones crushed post-ethanol showing greater colony counts. Cultures from intact stones immersed in ethanol for 10–20 minutes all showed no growth, with robust lawn growth from stones of the same cohort that were crushed prior to culturing. The above held true whether saline or water was used. Both the 70% ethanol and the autoclave eliminated viable *E. coli*, while UV demonstrated lawn growth equivalent to control.

**Conclusions:** We present a straightforward and reproducible method of producing *in vitro* kidney stone phantoms with viable internal and external *E. coli*, lowering the barrier for bench research on infected kidney stones. Immersion in 70% ethanol for at least 10 minutes eliminates surface *E. coli* while leaving internal bacteria unharmed, possibly mirroring the stone of the patient prescribed culture-driven antibiotics for an infection-associated stone.

**Funding:** N/A

## Abstract 45

### Inhibition of the mitochondrial chaperone TRAP1 disrupts kidney cancer cell survival

*Roman Isakov, Mark Woodford*
SUNY Upstate Medical Center, Syracuse, NY

**Introduction:** The molecular chaperone TNF-receptor-associated protein 1 (TRAP1) is a master regulator of mitochondrial metabolism and apoptosis and is often overexpressed in cancer. Insensitivity to apoptotic signaling underlies the pathogenesis of cancer, though the impact of TRAP1 on kidney cancer survival has not been explored. TRAP1 activity is modulated by post-translational modifications, which are often deregulated in disease. The proto-oncogene tyrosine kinase c-Abl is hyperactive in clear cell renal cell carcinoma (ccRCC), though the mitochondrial targets of c-Abl are unknown.

**Methods:** We have used established ccRCC cell lines to determine the impact of TRAP1 on ccRCC survival. We further evaluated TRAP1 phosphorylation using transient expression of phosphomutants and observed the impact of targeted disruption of TRAP1 phosphorylation on cell survival in HAP1, mouse embryonic fibroblast (MEF), and ccRCC cells.

**Results:** We observed elevated TRAP1 expression in the most common subtype of kidney cancer, ccRCC, and inhibition of TRAP1 in ccRCC-induced apoptosis. We found that c-Abl-mediated phosphorylation of TRAP1 antagonized apoptosis by promoting TRAP1 binding to the apoptosis effector cyclophilin D (CypD). Inhibitor-sensitive c-Abl-mediated TRAP1 phosphorylation was enriched in cancers, suggesting a direct link to cancer cell survival. Co-targeting TRAP1 and c-Abl displayed drug synergy, suggesting a potentially viable therapeutic strategy for ccRCC.

**Conclusions:** Here we observed that elevated TRAP1 expression and increased c-Abl-mediated phosphorylation drove the pro-survival role of TRAP1 in ccRCC. Therefore, combination c-Abl and TRAP1-specific inhibition merits continued evaluation.

**Funding:** N/A

## Abstract 38

### To bego or not to bego: Updating kidney stone phantoms

*Stephen Hassig, Christopher Wanderling, Thomas Osinski, Scott Quarrier, Mitchell Hoestermann, Connor Bittlingmaier, Rajat Jain*
University of Rochester Medical Center, Rochester, NY

**Introduction:** BegoStone is a widely accepted phantom for kidney stone bench experimentation. However, BegoStone with water has limitations: the mixture is too hard, homogenous, and lacks organic components that real stones possess. This study assessed the effect of BegoStone formulations on tensile fracture strength (TFS) and density in Hounsfield units (HU).

**Methods:** Ratios of BegoStone with water, saline, albumin (protein), agar (sugars), and/or calcium oxalate were varied. Mixtures were set in cylindrical molds and then compressed slowly on an Instron machine (500N sensor) to obtain TFS. Mean and standard deviation were calculated (Table 1). Twelve formulas had HU and architecture assessed with micro-CT (VivaCT-40).

**Results:** Over 400 cores were fractured from 21 formulations. Some required more than the maximum 500N, so these were water-soaked and retested, showing significant reduction in TFS. Formulas fell within the physiologic range of TFS at 0.6–4.8 MPa. Increasing water or saline fraction inhibited setting, agar powder yielded softer stones, and oxalate effect varied. Micro-CT demonstrated HU of 535–1538 (Figure 1).

**Conclusions:** BegoStone and water alone inaccurately replicate kidney stones in composition and testing. We demonstrated that varying the liquid and other components (protein, sugars, oxalate) yielded phantoms that approximated the TFS and HU of real stones, but with truer composition vs. current standards.

**Funding:** University of Rochester School of Medicine and Dentistry Faculty Council

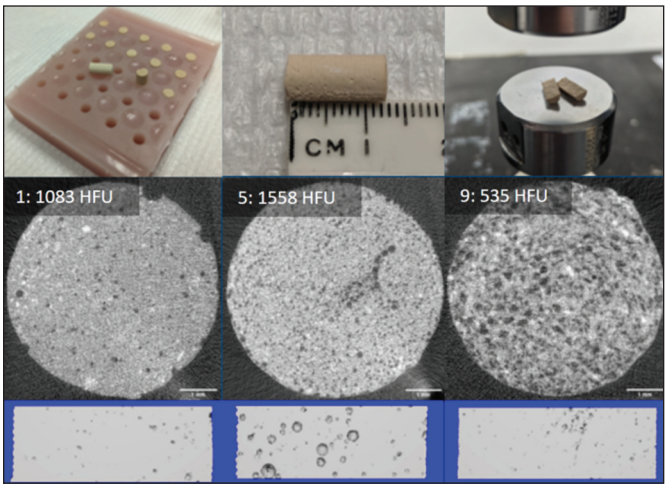


**Abstract 38. Figure 1.** Micro-CT demonstrated Hounsfield units of 535–1538.

**Abstract 46. Table 1. Twenty-one different formulas and over 400 total cores were fractured**

| Formula | Dry/wet | BegoStone | Water | Saline | Albumin | Agar | Oxalate | Mean tensile fracture strength (MPa) | Standard deviation (MPa) |
|---|---|---|---|---|---|---|---|---|---|
| 1 | D | 66 | 31.5 | | 2.5 | | | 3.106735 | 0.595502 |
| 2 | D | 72 | 25.5 | | 2.5 | | | 3.521613 | 0.772067 |
| 3 | D | 73 | 24.5 | | 2.5 | | | 3.757059 | 0.58644 |
| 4 | D | 81 | 16.5 | | 2.5 | | | >500N | >500N |
| 4 | W | 81 | 16.5 | | 2.5 | | | 2.66 | 0.347 |
| 5 | D | 82 | 15.5 | | 2.5 | | | >500N | >500N |
| 6 | D | 66 | 31.5 | | | 2.5 | | 3.105484 | 0.589519 |
| 7 | D | 72 | 25.5 | | | 2.5 | | 3.034286 | 0.632073 |
| 8 | D | 73 | 24.5 | | | | | >500N | >500N |
| 8 | W | 73 | 24.5 | | | | | 1.3 | 0.239 |
| 9 | D | 63.5 | 31.5 | | | 5 | | 2.54 | 0.28043 |
| 10 | D | 70.5 | 24.5 | | | 5 | | 2.955333 | 0.368372 |
| 11 | D | 79.5 | 15.5 | | | 5 | | WNM | WNM |
| 12 | D | 50 | 50 | | | | | WNS | WNS |
| 13 | D | 67 | 33 | | | | | >500N | >500N |
| 13 | W | 67 | 33 | | | | | 1.27 | 0.184 |
| 14 | D | 75 | 25 | | | | | >500N | >500N |
| 14 | W | 75 | 25 | | | | | 2.08 | 0.225 |
| 15 | D | 50 | | 50 | | | | WNS | WNS |
| 16 | D | 67 | | 33 | | | | 3.661 | 0.573305 |
| 17 | D | 75 | | 25 | | | | >500N | >500N |
| 17 | W | 75 | | 25 | | | | 1.47 | 0.165 |
| 18 | D | 63.5 | 31.5 | | 2.5 | | 2.5 | 2.743333 | 0.304292 |
| 19 | D | 70.5 | 24.5 | | 2.5 | | 2.5 | >500N | >500N |
| 19 | W | 70.5 | 24.5 | | 2.5 | | 2.5 | 1.63 | 0.201 |
| 20 | D | 40 | 20 | | | | 40 | WNM | WNM |
| 21 | D | 33 | 33 | | | | 33 | 2.180909 | 0.419344 |

Some formulations were too hard for 500N to fracture (>500N), some formulations would not mold (WNM) due to viscosity, and some formulations would not set (WNS). Formulas that were too hard were soaked for 12 hours in deionized water (W) and retested.